

LA-4901

③. 3

CIC-14 REPORT COLLECTION
**REPRODUCTION
COPY**

Evaluated Neutron-Induced
Gamma-Ray Production Cross Sections
for ^{239}Pu and ^{240}Pu



los alamos
scientific laboratory
of the University of California
LOS ALAMOS, NEW MEXICO 87544

This report was prepared as an account of work sponsored by the United States Government. Neither the United States nor the United States Atomic Energy Commission, nor any of their employees, nor any of their contractors, subcontractors, or their employees, makes any warranty, express or implied, or assumes any legal liability or responsibility for the accuracy, completeness or usefulness of any information, apparatus, product or process disclosed, or represents that its use would not infringe privately owned rights.

Printed in the United States of America. Available from
National Technical Information Service
U. S. Department of Commerce
5285 Port Royal Road
Springfield, Virginia 22151
Price: Printed Copy \$3.00; Microfiche \$0.95

LA-4901

UC-34

ISSUED: July 1972



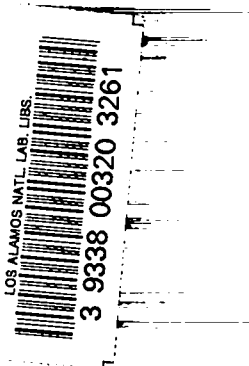
los alamos
scientific laboratory
of the University of California
LOS ALAMOS, NEW MEXICO 87544

Evaluated Neutron-Induced
Gamma-Ray Production Cross Sections
for ^{239}Pu and ^{240}Pu

by

R. E. Hunter*

L. Stewart



*Mr. Hunter was a consultant to the Los Alamos Scientific Laboratory at the time this report was written.

EVALUATED NEUTRON-INDUCED GAMMA-RAY PRODUCTION CROSS SECTIONS
FOR ^{239}Pu AND ^{240}Pu

by

R. E. Hunter and L. Stewart

ABSTRACT

The gamma-ray production cross sections produced by neutron interactions from 10^{-5} eV to 20 MeV have been evaluated for ^{239}Pu and ^{240}Pu . The data were prepared for input into the ENDF/B format. Below 1 MeV, the "prompt" fission and radiative capture spectra are included along with the gammas from inelastic scattering. Above 1 MeV, the total gamma-ray production cross sections from all nonelastic processes are input as a single reaction because the experimental measurements did not discriminate between the individual reaction channels. At all energies, all gamma rays are assumed to be emitted isotropically.

I. INTRODUCTION

The data required for radiation shielding, heating, and gamma-ray transport calculations cover the incident neutron energy range from 10^{-5} eV to 20 MeV. Yet, few experimental measurements exist on ^{239}Pu in which the gamma rays are observed and the results are reported in units which lend themselves to useful interpretation; on ^{240}Pu , there are no data at all. For a fissile nuclide such as ^{239}Pu , three types of measurements are available.

First, coincidence techniques have been employed in pulsed-beam experiments to determine the gamma-ray spectrum associated with fission events (over a given time after fission) at thermal energy. These data are reported as the number of gammas per fission over specified gamma energy intervals.¹ When normalized to the thermal fission cross section for ^{239}Pu , these data provide the absolute cross sections required for input calculations.

Second, the thermal capture spectrum for ^{239}Pu has not been observed, although Journey and Sheline² measured the line spectra at thermal for $E_\gamma > 3.3$ MeV and provided these data in terms of cross sections. These discrete lines could sometimes be

ascribed to the fission process and sometimes to radiative capture, but few of the gamma rays could be uniquely assigned. It is reasonable to assume that the discrete lines would account for only a small part of the total gamma-ray production cross section because prompt fission gammas did not appear as lines. These data, therefore, provide only a check on the total gamma-ray production cross section calculated, assuming a radiative capture spectrum which is then folded into the measured fission-gamma spectrum normalized to the thermal fission cross section.

Third, for neutron energies above 1 MeV, Drake et al.³ and Nellis and Morgan⁴ have measured cross sections on ^{239}Pu . They did not attempt to separate the gammas due to radiative capture, fission, inelastic scattering, (n,2n), or (n,3n) processes. The results are presented as a continuum spectrum with a 500-keV low-energy detector cutoff. The extrapolation to $E_\gamma = 0$, to obtain the integral cross sections, presents significant problems. The interpretation of these results is discussed in Section II.C.

II. ^{239}Pu

As discussed previously, data on ^{239}Pu are sparse. In particular, no measurements are available on the angular distributions of the gamma rays produced by specific reactions with neutrons on ^{239}Pu , although Nellis and Morgan⁴ found the total gamma-ray production cross-section angular distributions to be isotropic to within $\pm 10\%$ at incident neutron energies of 1.09, 4.0, and 14.8 MeV. In the absence of data to the contrary, all processes are assumed to be isotropic.

Because the absolute cross sections at some energies must be obtained by using multiplicities*, although measurements at other energies are reported in barns/MeV, it seemed desirable for discussion to separate the neutron energy range as follows: the thermal range up to the onset of inelastic scattering, the region from the inelastic threshold up to 1.09 MeV, and 1.09 to 20 MeV. Several total gamma-ray production spectra measurements have been made from 1.09 to 14.8 MeV; these and other data will be discussed later.

A. 10^{-5} eV to ~ 8 keV

The fission, radiative capture, and elastic-scattering cross sections go through many resonances, and it is reasonable to assume that the gamma-ray spectrum changes quite rapidly with incident neutron energy over the fission and capture resonances. Neither experimental spectra nor theoretical calculations have been reported for the resonant-energy region.

1. Radiative Capture. The thermal radiative capture spectrum was generated using the results of Orphan et al.⁵ on Hf as a starting point. Their report shows an extrapolation of the "continuum" region to zero cross section at low gamma-ray energies; in this report, a contribution to the continuum was arbitrarily assigned down to zero energy. Further, the results are renormalized on the basis of the difference between the binding energies of ^{239}Pu and Hf, obtaining in the final analysis approximately the same multiplicity for both elements. The probability distribution so obtained (normalized to one photon per capture) is shown in Fig. 1.

* The gamma-ray multiplicity is defined as the number of gamma rays emitted per reaction.

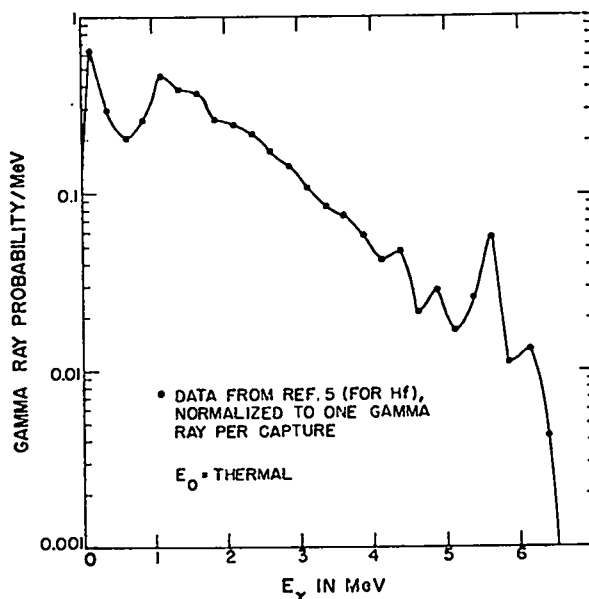


Fig. 1. Probability for production of photons as a function of E_γ due to capture by ^{239}Pu (normalized to 1 gamma ray per capture) for thermal neutrons. Values are obtained from measurements on hafnium,⁵ adjusted to the binding energy of ^{239}Pu .

2. Fission. Using coincidence (with the fission fragment) and time-of-flight techniques, the fission gamma-ray spectrum has been observed¹ at thermal for ^{235}U and ^{239}Pu ; in the same experiment, ^{252}Cf , which fissions spontaneously, was studied. Earlier measurements of the yields and spectra on ^{235}U (Ref. 6, 7) and ^{252}Cf (Ref. 8) were confirmed, although some differences were reported. Peelle and Mainschein⁹ have recently reanalyzed and reported the earlier data of Mainschein et al.⁶

Many authors have treated the theory of fission and some have included the yield and total energy of the gamma rays in their analyses. As Peelle and Mainschein⁹ discuss, however, the definition of "prompt gamma-ray spectra" depends upon the experimental techniques employed and, all too often, the times associated with the gamma-ray emission also depend upon the resolving time of the detectors as well as the time delay between the fission process and the emission of the gamma ray. In one measurement,¹⁰ an upper limit of 0.05 nsec was reported for those protons emitted promptly after scission; there is no evidence for photon emission before scission. Following the gamma rays emitted

after scission, isomeric transitions in the fission fragments themselves do produce gamma rays, but these are primarily of low energy and contribute only a small percentage of the total number of photons. It is generally agreed that the total energy of the photons emitted directly after scission (prompt) is essentially the same (7-8 MeV) as that from the fission products produced by β decay of the initial fragments.

Relying heavily on the data of Verbinski and Sund,¹ and extrapolating to zero energy, a value of 7.1 MeV/fission for ^{239}Pu was obtained for those gammas emitted in ~ 100 nsec following fission. (Obviously this choice of time interval is by no means unique.) No measurement of the time dependence of the emission of photons from ^{239}Pu is available. Also, no measurements have been made showing the energy dependence, although James¹¹ recommends a constant value of 8.0 ± 1.5 MeV/fission, based on the energy dependence of related fission parameters. In the absence of data to the contrary, a constant value of 7.1 MeV/fission was chosen for this evaluation.

Measurements on the fission gamma-ray spectrum observed at thermal energy are shown in Fig. 2. The ordinate gives the absolute number of gamma rays per MeV per fission and, therefore, integrates to the measured multiplicity after extrapolating to $E_\gamma = 0$.

For this evaluation, only the recent measurements by Verbinski and Sund¹ were considered since their experimental techniques are far superior to those employed by Maienschein in the early 50's. Although the earlier data indicate an average fission gamma energy ~ 1 MeV larger, it is possible that the detector used was not entirely insensitive to neutron events and thereby recorded an unmeasurable background. Although this hypothesis has not been verified experimentally, the data of Verbinski and Sund were chosen rather than an average of the two measurements. The probability distribution was normalized to one photon per fission, and this spectrum was assumed to apply up to the 1.09-MeV region; that is, the spectral function is independent of incident neutron energy.

3. Summary. To obtain the gamma-ray production cross sections, the probability distributions for fission and capture must be multiplied by the

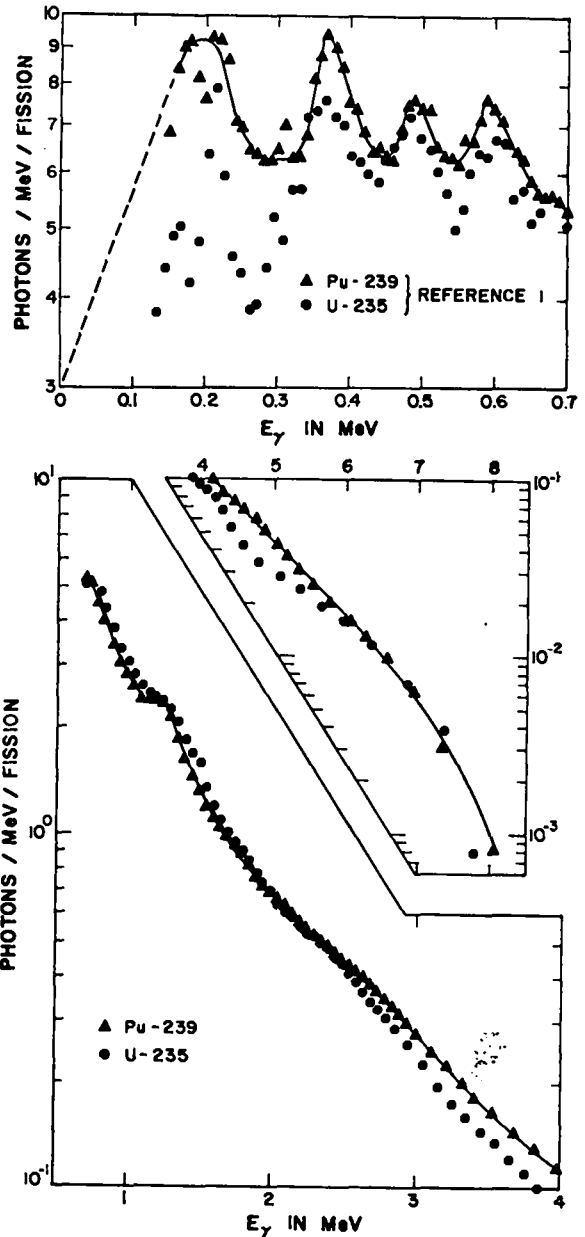


Fig. 2. Photons per MeV per fission for ^{239}Pu and ^{235}U for thermal neutrons as a function of E_γ . The experimental points of Verbinski and Sund¹ are compared with the evaluated data for ^{239}Pu , shown as a smoothed curve.

appropriate neutron cross sections and the correct multiplicities at each neutron energy. This ensures that any changes in the neutron cross sections and the proper weighting functions will automatically be applied to the calculated gamma-ray production cross sections. This method also allows the user to handle these low-energy and resonance-region cross

sections in any manner he deems appropriate for the problem under study.

The spectral functions for radiative capture and fission over the resonance region probably vary rapidly with energy. Additionally, of course, it is unreasonable to expect p-wave capture to produce the same "average" spectral functions as an s-wave resonance. Even the small "background" components may have different spectra. With no experimental information, however, both the capture and fission γ -ray spectra are assumed to be independent of incident neutron energy up to 1.09 MeV, except for modifications to the capture spectra to conserve total energy.

B. 8 keV to 1.09 MeV

1. Radiative Capture. At the lowest energy, the thermal capture spectrum was employed. At 1.09 MeV, the capture spectrum was modified somewhat arbitrarily to give the total energy required; that is, $E_0 + E_b$ or 7.52 MeV. The normalized spectrum is shown in Fig. 3.

2. Fission. The gamma-ray energy distribution for thermal fission was used at all incident neutron energies up to $E_0 = 1.09$ MeV. Since the gamma-ray energy per fission is assumed to be invariant with incident neutron energy,⁵ the multiplicity is also assumed to be constant from thermal up to 1.09 MeV.

3. Inelastic Scattering. The gamma-ray spectra for inelastic scattering were calculated using the excitation cross sections by Hunter et al.¹² for the individual levels and the continuum contribution. Once excited, the residual nucleus loses its energy by the emission of one or more gamma rays. Using statistical theory and the branching ratios compiled by Lederer et al.,¹³ the absolute cross sections were calculated for the production of gamma rays of energies $E_{\gamma 1}$. This, in turn, produced a gamma-ray multiplicity at each incident neutron energy. This method ensured that, consistent with the inelastic cross sections in Ref. 12, the total gamma-ray energy would be equal to the incident neutron energy minus the energy carried away (on the average) by the inelastically scattered neutrons.

For incident neutron energies above 300 keV, Hunter et al.¹² represent an increasing percentage of the final state neutron energy distribution

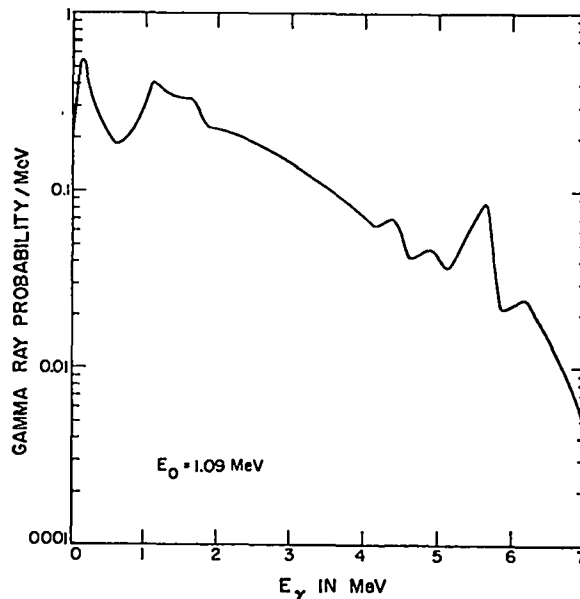


Fig. 3. Probability for production of photons as a function of E_γ , due to capture by ^{239}Pu (normalized to 1 gamma ray per capture), for an incident neutron energy of 1.09 MeV.

by an evaporation model. At 1.09 MeV, the entire neutron cross section is assigned to this continuum process, therefore the excitation for individual levels could not readily be determined. A continuum distribution of gamma rays was calculated based on the total energy available from kinematics; that is $\bar{E}_\gamma = E_0 - \bar{E}_n$. A large cross section for the production of the 8-keV gamma ray was assigned since most of the cascades proceed through the 8-keV level, and the remaining energy was then distributed in the gamma-ray continuum after small probabilities were assigned to a few discrete gammas below 300 keV.

The multiplicity at 1.09 MeV was determined by extrapolating a smooth curve from data obtained at lower energies. This, in turn, permitted calculation of an average gamma-ray energy for the continuum spectrum. The continuum distribution was then calculated using the evaporation model:

$$F(E_\gamma) = N E_\gamma e^{-E_\gamma/T_\gamma}, \quad (1)$$

where N is the normalization constant and $T_\gamma = \bar{E}_\gamma^c/2$; \bar{E}_γ^c is the average gamma-ray energy for the continuum. The probability distribution was

cut off at $E_\gamma = 1$ MeV and normalized over the energy range from $E_\gamma = 0$ to $E_\gamma = 1.0$ MeV.

Up to 300 keV, the inelastic scattering gamma rays were input as discrete lines. The multiplicities for the three lowest-energy gamma rays (7.85, 49.41, and 57.27 keV) are reproduced in Table IV (at the end of this report) as examples. Above 300 keV, the gamma rays are tabulated as the sum of discrete lines with a continuum contribution, the continuum being tabulated at three incident neutron energies: 300, 500, and 1090 keV. Linear-linear interpolation is recommended for the multiplicities at all neutron energies.

These data represent the inelastic gamma-ray spectra reasonably well. If, however, one chooses significantly different inelastic neutron cross sections, such as those which appeared in ENDF/B Version II and were discussed by Prince,¹⁴ then the gamma-ray production cross sections chosen here would probably require significant modifications. Prince's inelastic cross sections are about twice as large at a few MeV as those in all other evaluated libraries available at this time.

C. 1.09 to 20 MeV

Drake et al.³ and Nellis and Morgan⁴ have reported measurements of the total gamma-ray spectra from 1.09 to 14.8 MeV. Drake et al. give the cross sections in barns over 250-keV intervals with accuracies of 10%, whereas Nellis and Morgan report broader energy intervals of 500 keV and quote a 20% uncertainty. Such data present the evaluator with a corresponding uncertainty (and/or flexibility) in drawing smooth curves to represent the gamma-ray spectra. In addition, as noted in the Introduction, the extrapolation to $E_\gamma = 0$ presents rather serious problems and uncertainties. For example, this extrapolation of the experimental measurements alone accounts for 35-46% of the total production cross section, as is clearly indicated in Tables VII and XIII.

Other evaluations of gamma-ray production cross sections often show larger values in the MeV range than those quoted here, the major difference being in the method chosen for extrapolation below $E_\gamma = 500$ keV. For example, note that a straight-line extrapolation on the energy spectra could double or even triple the total integral in barns, depending upon the slope at the point chosen for

extrapolation. Therefore a study was made of the measurements of Drake¹⁵ on ^{235}U , which extend down to a low-energy cutoff of 250 keV and thereby cover half the energy range over which the ^{239}Pu data require extrapolation. Drake's data indicate that the gamma-ray yield between 250 and 500 keV is only slightly larger than the measured yield between 500 and 750 keV.

Further, the shapes of the gamma-ray production cross sections above 1 MeV are similar for ^{235}U and ^{239}Pu . Remembering that most gammas come from fission and that the fission gamma-ray spectrum is assumed to be independent of incident neutron energy, it seemed reasonable to extrapolate the ^{239}Pu spectra below 500 keV using the shapes measured by Drake¹⁵ for ^{235}U .

The uncertainty in the absolute magnitude of the spectra is constrained by requiring energy conservation:

$$\int_0^\infty E_\gamma \sigma_{\gamma\text{prod}}(E_\gamma) dE_\gamma = \bar{E}_{\gamma f} \sigma_{n,f} + (E_0 - \bar{E}_n) \sigma_{n,n} + (E_0 + E_b) \sigma_{n,\gamma} + (E_0 + Q_{2n} - 2\bar{E}_{2n}) \sigma_{n,2n} + (E_0 + Q_{3n} - 3\bar{E}_{3n}) \sigma_{n,3n} \quad (2)$$

where $\bar{E}_{\gamma f}$ is the average total energy of the gamma rays from fission (taken to be 7.1 MeV); \bar{E}_n , \bar{E}_{2n} , and \bar{E}_{3n} are average energies carried off by neutrons in inelastic, (n,2n), and (n,3n) processes; E_b is the binding energy for capture (6.43 MeV); and Q_{2n} and Q_{3n} are the Q-values for the (n,2n) and (n,3n) processes (-5.66 and -12.65 MeV, respectively). The absolute scales of the various gamma-ray distributions were checked against Eq. (2); the differences were typically a few percent, always within experimental error, and were never greater than 10%.

The gamma-ray cross sections and spectra were extended to $E_0 = 20$ MeV by extrapolating the normalized distributions at each gamma-ray energy as a function of incident neutron energy and drawing smooth curves through the experimental results. The absolute values were also checked using Eq. (2).

The experimental data along with the evaluated curves are shown in Figs. 4-6 (at end of report).

These results are given as absolute cross sections in barns/MeV as a function of E_γ . They correspond to the total gamma-ray production cross sections from all nonelastic collisions.*

III. ^{240}Pu

A. 10^{-5} eV to 43 keV

Lacking experimental data on ^{240}Pu , the gamma-ray production cross sections were generated from measurements on other isotopes, assuming the nuclear systematics aren't too different.

Since the gamma-ray spectra from fission are similar for a number of isotopes, the spectrum for ^{239}Pu (Fig. 2) was used without modification for ^{240}Pu . Further, the total gamma-ray energy associated with prompt fission was found to be roughly the same for ^{239}Pu and ^{235}U ; therefore, the total energy and the fission multiplicity obtained for ^{239}Pu were again used for ^{240}Pu .

The capture gamma-ray spectrum for ^{240}Pu is expected to be somewhat different from that for ^{239}Pu since ^{240}Pu is an even-even nuclide. Therefore, the capture gamma-ray spectrum was based on measurements on ^{238}U by John and Orphan.¹⁶ They measured the gamma rays emitted over a range of incident neutron energies and resonances from 5.6 eV to 101.9 keV. These data were averaged and then normalized to produce the spectrum shown in Fig. 7. The calculated thermal multiplicity was based on the average gamma-ray energy obtained from the curve shown in Fig. 7 and the binding energy for ^{240}Pu .

B. 43 keV to 1.09 MeV

The fission spectrum and multiplicity are assumed to be constant up to 1.09 MeV. The thermal capture gamma-ray spectrum was used up to 43 keV and then hardened to account for the increased energy available at 1.09 MeV, while keeping the capture multiplicity essentially constant. Linear interpolation should be used between energy points. The resulting normalized curve is shown in Fig. 8.

The gamma-ray production cross section from inelastic scattering was treated in the manner described for ^{239}Pu . Again, the level excitation cross sections were taken from the evaluation of Hunter et al.¹² in order to calculate the production cross sections for gamma emission at selected neutron energies up to 1.09 MeV. The only difference between ^{239}Pu and ^{240}Pu arises from the much lower level density for ^{240}Pu ; hence, level excitation cross sections were given in Ref. 12 all the way to $E_0 = 1.09$ MeV.

C. 1.09 to 20 MeV

At $E_0 = 1.09$ MeV, the total gamma-ray production cross section was calculated from the spectra and multiplicities given above using the neutron cross sections given by Hunter et al.¹² Comparisons were made with the gamma-ray spectrum for ^{239}Pu , after adjusting the magnitude to give energy balance for ^{240}Pu . Agreement was very good.

At $E_0 = 2.1, 3.0, 4.0, 5.0, 6.0, 7.5, 14.8,$ and 20 MeV, the energy balance for ^{240}Pu was calculated using Eq. (2) with $\bar{E}_{\gamma f} = 7.1$ MeV and $E_b = 5.57$ MeV. Values for the other neutron parameters were taken from Hunter et al.¹² Values of the integral were adjusted (on absolute scales) using the gamma-ray production cross sections for ^{239}Pu to obtain corresponding curves for ^{240}Pu ; the results are shown in Figs. 9-11.

IV. RESULTS

The final results are tabulated to facilitate input into a library file and ready incorporation of subsequent changes. First, the total gamma-ray production cross sections in barns, integrated over E_γ , are plotted as a function of incident neutron energy above 1 MeV for ^{239}Pu and ^{240}Pu in Fig. 12. Note that these integrals vary from ~ 16 to 25 b.

Linear-linear interpolation is recommended but it is recognized that some users may require other interpolation schemes as dictated by particular processing codes; in such cases, additional datum points (from the microscopic curves) and/or re-normalization of probabilities may be required to ensure proper representation of the data. Note also that the energy mesh used for $\sigma(E_\gamma)$ and $P_\gamma(E_\gamma)$ does not coincide with the fine structure for the gamma-ray probability distribution for radiative capture for ^{239}Pu . The error involved in failing

* Note that these gamma-ray production cross sections are not uniquely related to a specific neutron cross section. Therefore, it is not physically meaningful to try to calculate multiplicities using the total neutron nonelastic cross section.

to represent those peaks precisely is considerably less than the uncertainty in the gross distribution, because that curve was based on the radiative capture process for hafnium, and therefore may be systematically different from similar measurements on ^{239}Pu .

Again note that all distributions are given in units of probability per MeV or barns/MeV except for discrete level information which is presented as probabilities for the production of gamma rays of discrete energies, $E_{\gamma i}$. Quoting probability per MeV for a discrete level is physically meaningless without some specification of line width and shape.

The results for both ^{239}Pu and ^{240}Pu are presented in Tables I through XIII at the end of this report.

V. DISCUSSION

Malenschein et al.,⁶ Rau,⁷ Peelle and Maienschein,⁹ and Maienschein¹⁷ have studied extensively the gamma rays produced in thermal neutron-induced fission of ^{235}U . Additional work is detailed in Maienschein's references.¹⁷ Experimental information on ^{239}Pu is sparse, and data on ^{240}Pu are nonexistent. The gamma rays produced within 50-100 nsec after fission are most often called "prompt" and have an average total energy per fission of ~ 7.1 MeV. At later times, gamma rays which correspond to the isomeric transitions in the initial fragments themselves are emitted; these account for only a small part of the total energy and the total number of gamma rays. At still later times, another 7-8 MeV per fission (on the average) is carried off by gamma rays, but the total integration must be performed over long times, as the gamma rays are emitted from the fission products formed in the beta-decay chains. The emission time of a given photon will then be determined by the cumulative half-lives of all the daughter nuclides produced in sequential beta decay.

For this report, all capture, prompt fission, and inelastic processes are assumed short-lived; that is, the gamma rays are emitted within ~ 100 nsec. Hopefully, this assumption is reasonably valid for the data used here. Note, however, that the spectra for prompt fission should be "harder" than the the photon spectra produced at later times (i.e., the fission-product gamma rays) even though the total energy is essentially the same in each case.

For many reactor problems, the latter spectra would be of equal importance because, once equilibrium is reached, the fission products become a continuous gamma-ray source. Perhaps at some later date, the time dependence of the fission gamma-ray spectra may be considered for input calculations.

The dependence of the fission gamma-ray spectrum on incident neutron energy is not known for any of the fissionable isotopes of interest. Neither has the time dependence of the fission gammas been established above thermal energy.

The gamma-ray angular distributions for all reactions are assumed to be isotropic. Although little direct experimental information is available, the degree of anisotropy seems to be much smaller than observed for fission neutrons, that is, $< 10\%$ for incident neutrons above 1 MeV.

ACKNOWLEDGMENTS

We gratefully acknowledge helpful discussions with many people about various aspects of this evaluation effort. In particular, we appreciate the contributions of E. T. Journey, R. K. Sheline, H. T. Motz, and P. P. Whalen. T. L. Talley and D. W. Watkins contributed many helpful comments on the presentation of these results. We thank R. J. LaBauve for his splendid cooperation and assistance in preparing these data for the ENDF/B files. Finally, without the support and encouragement of C. C. Cremer and D. R. Harris, we would not have embarked on this program.

REFERENCES

1. V. V. Verbinski and R. E. Sund, "Measurement of Prompt Gamma-Rays from Thermal-Neutron Fission of ^{235}U and ^{239}Pu , and from Spontaneous Fission of ^{252}Cf ," General Atomic report GA-9148 (1969).
2. E. T. Journey and R. K. Sheline, private communication.
3. D. M. Drake, J. C. Hopkins, C. S. Young, and H. Condé, "Gamma-Ray-Production Cross Sections for Fast Neutron Interactions with Several Elements," Nucl. Sci. Eng. 40, 294 (1970).
4. D. O. Nellis and I. L. Morgan, "Gamma-Ray Production Cross Sections for U^{235} , U^{238} , and Pu^{239} ," Texas Nuclear Corp. report ORO-2791-17 (1966); also reported in P. S. Buchanan, "A Compilation of Cross Sections and Angular Distributions of Gamma Rays Produced by Neutron Bombardment of Various Nuclei," Texas Nuclear Corp. report ORO-2791-28 (1969).
5. V. J. Orphan, N. C. Rasmussen, and T. L. Harper, "Line and Continuum Gamma-Ray Yields from Thermal-Neutron Capture in 75 Elements," General Atomic report GA-10248 (1970).
6. F. C. Maienschein, R. W. Peelle, W. Zobel, and T. A. Love, "Gamma Rays Associated with Fission," Proc. U. N. Intern. Conf. Peaceful Uses At. Energy, 2nd, Geneva, 1958, 15, 366 (1958).
7. F. E. W. Rau, "Ausbeute an Prompter Gammastrahlung bei Spaltugn von Uran 235 durch Thermische Neutronen," Ann. Physik (7)10, 252 (1963).
8. H. R. Bowman and S. G. Thompson, "The Prompt Radiations in the Spontaneous Fission of Californium-252," Proc. U. N. Intern. Conf. Peaceful Uses At. Energy, 2nd, Geneva, 1958, 15, 212 (1958).
9. R. W. Peelle and F. C. Maienschein, "The Absolute Spectrum of Photons Emitted in Coincidence with Thermal-Neutron Fission of Uranium-235," Oak Ridge Natl. Lab. report ORNL-4457 (1970).
10. G. V. Val'skii, D. M. Kaminkev, G. A. Petrov, and L. A. Popeko, "Concerning the Emission Times of γ -Quanta as a Result of Fission," At. Energ. (USSR) 18, 223 (1965); Soviet J. of At. Energ. 18, 279 (1965).
11. M. F. James, "Energy Released in Fission," J. Nucl. Energy 23, 517 (1969).
12. R. E. Hunter, J. J. H. Berlijn, and C. C. Cremer, "Neutron Cross Sections for ^{239}Pu and ^{240}Pu in the Energy Range 1 keV to 14 MeV," LASL report LA-3528 (1968).
13. C. M. Lederer, J. M. Hollander, and I. Perlman, Table of Isotopes, 6th Ed., John Wiley & Sons: New York (1967).
14. A. Prince, "Analysis of High-Energy Neutron Cross-Sections for Fissile and Fertile Isotopes," Proc. 2nd Intern. Conf. Nuclear Data for Reactors, Helsinki, Vol. II, 825 (1970).
15. D. M. Drake, "Inelastic Neutron Scattering and Gamma Production from Fast-Neutron Bombardment of ^{235}U ," Nucl. Phys. A133, 108 (1969).
16. J. John and V. J. Orphan, "Gamma Rays from Resonant Capture of Neutrons in ^{238}U ," General Atomic report GA-10186 (1970).
17. F. C. Maienschein, "Prompt-Fission Gamma Rays," Engineering Compendium on Radiation Shielding, Vol. I, Springer-Verlag: New York (1968), p.77, 78.

TABLE I

FISSION GAMMA-RAY PROBABILITY
FOR Pu-239 AND Pu-240
(Normalized to one photon per fission)
 $E_0 = 10^{-5}$ eV to 1.09 MeV.

E_γ (MeV)	$P(E_\gamma)$ Prob/MeV	E_γ (MeV)	$P(E_\gamma)$ Prob/MeV	E_γ (MeV)	$P(E_\gamma)$ Prob/MeV
0.0	0.3644	0.58	0.8894	3.0	0.0341
0.05	0.5065	0.59	0.9389	3.25	0.0264
0.10	0.6856	0.60	0.9141	3.5	0.0210
0.15	0.8894	0.645	0.7412	3.75	0.0169
0.175	1.118	0.66	0.6955	4.0	0.0140
0.20	1.136	0.68	0.6856	4.25	0.0110
0.21	1.124	0.70	0.6609	4.5	0.0086
0.225	1.038	0.75	0.5991	4.75	0.0069
0.25	0.8586	0.85	0.4756	5.0	0.0055
0.275	0.7844	0.95	0.3669	5.25	0.0044
0.3	0.7783	1.0	0.3372	5.5	0.0035
0.34	0.8586	1.05	0.3113	5.75	0.0027
0.36	1.087	1.1	0.3002	6.0	0.0021
0.37	1.161	1.2	0.2940	6.25	0.0016
0.39	1.044	1.25	0.2779	6.5	0.0012
0.41	0.8894	1.3	0.2569	6.75	0.00091
0.43	0.8091	1.4	0.1952	7.0	0.00068
0.45	0.7783	1.5	0.1606	7.25	0.00049
0.47	0.8586	1.6	0.1359	7.5	0.00034
0.48	0.9265	1.7	0.1167	7.75	0.00023
0.49	0.9389	1.85	0.0951	8.0	0.00012
0.50	0.9018	2.0	0.0831	8.1	0.00010
0.52	0.8153	2.25	0.0674		
0.545	0.7783	2.5	0.0550		
0.57	0.8277	2.75	0.0436		

TABLE II

RADIATIVE-CAPTURE GAMMA-RAY PROBABILITY
FOR Pu-239(Normalized to one photon per capture)
 $E_0 = 10^{-5}$ eV to 8 keV.

E_γ (MeV)	P(E_γ) (Prob/MeV)	E_γ (MeV)	P(E_γ) (Prob/MeV)
0.0	0.106	2.25	0.234
0.1	0.549	2.50	0.195
0.2	0.510	2.75	0.154
0.3	0.343	3.00	0.125
0.4	0.271	3.25	0.0945
0.5	0.229	3.50	0.0796
0.6	0.209	3.75	0.0669
0.7	0.213	4.00	0.0488
0.8	0.231	4.25	0.0446
0.9	0.270	4.50	0.0308
1.00	0.345	4.75	0.0244
1.25	0.425	5.00	0.0212
1.50	0.374	5.50	0.0393
1.75	0.310	6.00	0.0117
2.00	0.254	6.50	0.0

TABLE III

RADIATIVE-CAPTURE GAMMA-RAY PROBABILITY
FOR Pu-239(Normalized to one photon per capture)
 $E_0 = 1.09$ MeV*.

E_γ (MeV)	P(E_γ) (Prob/MeV)	E_γ (MeV)	P(E_γ) (Prob/MeV)
0.0	0.0944	2.25	0.208
0.1	0.488	2.50	0.190
0.2	0.453	2.75	0.166
0.3	0.305	3.25	0.122
0.4	0.241	3.50	0.102
0.5	0.204	3.75	0.0892
0.6	0.186	4.00	0.0737
0.7	0.190	4.25	0.0662
0.8	0.206	4.50	0.0540
0.9	0.240	4.75	0.0471
1.00	0.307	5.00	0.0420
1.25	0.376	5.50	0.0727
1.50	0.331	6.00	0.0223
1.75	0.262	6.50	0.0135
2.00	0.223	7.00	0.0045
		8.0	0.0

*For E_0 of 8 keV to 1.09 MeV, interpolate between the probabilities given in Tables II and III. For E_0 above 1.09 MeV, use the gamma-ray production cross sections in Table VI.

TABLE IV

INELASTIC GAMMA-RAY MULTIPLICITIES*
FOR Pu-239

E_0 (keV)	$E_\gamma = 7.85$ (keV)	$E_\gamma = 49.41$ (keV)	$E_\gamma = 57.27$ (keV)
7.883	1.0	-	-
15.0	1.0	-	-
57.51	1.0	0.0	0.0
60.0	0.97	0.03	0.003
76.34	0.94	0.06	0.006
80.0	0.92	0.065	0.0065
100.0	0.92	0.071	0.007
164.43	0.92	0.071	0.007
180.0	0.92	0.071	0.007
286.69	0.92	0.071	0.007
300.0	0.92	0.071	0.007
500.0	0.92	0.071	0.007
1090.0	0.92	0.071	0.007

*Seven more discrete lines tabulated in the file are omitted here for convenience.

TABLE V

GAMMA-RAY MULTIPLICITIES FOR Pu-239
 $E_0 = 10^{-5}$ eV to 1.09 MeV

E_0 (keV)	Fission	Radiative Capture	Inelastic
Thermal	8.095	3.78	-
7.883	8.095	3.78	1.0
15.0	8.095	3.78	1.0
57.51	8.095	3.78	1.0
60.0	8.095	3.78	1.003
76.34	8.095	3.78	1.006
80.0	8.095	3.78	1.092
100.0	8.095	3.78	1.198
164.43	8.095	3.78	1.298
180.0	8.095	3.78	1.698
286.69	8.095	3.78	2.058
300.0	8.095	3.78	2.274
500.0	8.095	3.78	2.515
1090.0*	8.095	3.78	3.07

*For $E_0 > 1.09$ MeV, use the gamma-ray production cross sections in barns/MeV in Table VI.

TABLE VI

GAMMA-RAY PRODUCTION CROSS SECTIONS FOR ^{239}Pu , IN BARN/MeV

E_0 (MeV) \ E_γ (MeV)	1.09	2.1	3.0	4.0	5.0	6.0	7.5	14.8	20.0
0.0	8.68	10.77	8.77	13.18	12.84	11.71	11.52	9.67	8.60
0.1	15.89	12.25	10.79	16.23	14.86	13.85	13.92	12.71	12.24
0.2	17.82	13.92	13.07	18.56	17.43	16.19	16.71	15.47	15.07
0.3	17.34	15.21	15.70	21.50	20.33	18.34	20.45	18.42	17.56
0.4	16.39	16.50	17.37	22.61	23.21	20.19	22.37	20.45	19.76
0.5	14.72	16.40	17.63	22.82	23.75	20.77	23.05	21.19	20.57
0.6	12.56	15.71	17.02	20.58	21.92	19.80	22.08	20.26	20.54
0.7	10.42	14.03	14.21	16.23	17.11	16.28	18.24	18.60	19.36
0.8	8.44	12.15	11.58	12.47	13.37	12.00	12.77	15.20	17.48
0.9	6.87	10.17	9.64	10.04	10.16	9.07	9.89	12.25	14.78
1.0	5.69	8.59	8.16	7.96	8.02	7.22	8.06	10.13	12.36
1.25	3.77	5.43	5.52	4.87	5.02	4.85	5.18	6.64	7.85
1.50	2.62	3.45	3.94	3.43	3.58	3.71	3.75	4.66	5.54
1.75	1.90	2.29	3.09	2.65	2.69	3.15	2.75	3.27	3.81
2.00	1.43	1.63	2.39	2.16	2.28	2.58	2.05	2.40	2.76
2.25	1.08	1.23	1.80	1.81	1.85	2.06	1.58	1.76	1.96
2.50	0.860	0.958	1.29	1.43	1.44	1.60	1.21	1.29	1.40
2.75	0.675	0.754	0.930	1.09	1.07	1.26	0.931	0.953	1.01
3.00	0.535	0.603	0.605	0.760	0.760	0.974	0.730	0.709	0.732
3.25	0.422	0.476	0.414	0.531	0.593	0.745	0.561	0.550	0.552
3.50	0.333	0.378	0.325	0.385	0.470	0.576	0.442	0.424	0.426
3.75	0.265	0.300	0.255	0.304	0.372	0.432	0.344	0.329	0.331
4.00	0.210	0.238	0.202	0.241	0.296	0.336	0.264	0.258	0.263
4.25	0.168	0.190	0.162	0.192	0.235	0.252	0.209	0.204	0.208
4.50	0.132	0.149	0.129	0.152	0.186	0.197	0.159	0.161	0.169
4.75	0.106	0.120	0.102	0.121	0.148	0.154	0.125	0.127	0.134
5.00	0.083	0.095	0.080	0.095	0.118	0.123	0.095	0.099	0.108
5.50	0.053	0.059	0.050	0.060	0.075	0.078	0.057	0.064	0.068
6.00	0.033	0.038	0.032	0.038	0.047	0.050	0.035	0.040	0.044
6.50	0.021	0.024	0.020	0.024	0.030	0.031	0.022	0.025	0.028
7.00	0.013	0.015	0.013	0.016	0.019	0.019	0.014	0.015	0.018
8.00	0.0	0.0	0.0	0.0	0.0	0.0	0.0	0.0	0.0

TABLE VII

TOTAL GAMMA-RAY PRODUCTION CROSS SECTIONS FOR ^{239}Pu

E_0 (MeV)	$\int_0^{8 \text{ MeV}} \sigma(E_\gamma) dE_\gamma$ (barns)	$\int_0^{0.5 \text{ MeV}} \sigma(E_\gamma) dE_\gamma$ (barns)
1.09	17.08	7.86
2.1	19.28	7.15
3.0	19.89	7.01
4.0	23.27	9.68
5.0	23.65	8.48
6.0	22.34	8.48
7.5	23.10	9.07
14.8	23.71	8.23
20.0	25.09	7.90

TABLE VIII
RADIATIVE-CAPTURE GAMMA-RAY PROBABILITY FOR ^{240}Pu
(Normalized to one photon per capture)

$E_0 = 10^{-5}$ eV to 43 keV

E_γ (MeV)	P(E_γ) (Prob/MeV)	E_γ (MeV)	P(E_γ) (Prob/MeV)
0.0	0.0305	2.25	0.337
0.1	0.0459	2.50	0.192
0.2	0.0689	2.75	0.109
0.3	0.101	3.00	0.0651
0.4	0.150	3.25	0.0386
0.5	0.214	3.50	0.0242
0.6	0.283	3.75	0.0210
0.7	0.340	4.00	0.0261
0.8	0.398	4.25	0.0098
0.9	0.437	4.50	0.0035
1.0	0.462	4.75	0.0012
1.25	0.498	5.00	0.0003
1.50	0.584	5.5	0.0
1.75	0.505		
2.00	0.450		

TABLE IX
RADIATIVE-CAPTURE GAMMA-RAY PROBABILITY FOR ^{240}Pu
(Normalized to one photon per capture)

$E_0 = 1.09$ MeV

E_γ (MeV)	P(E_γ) (Prob/MeV)	E_γ (MeV)	P(E_γ) (Prob/MeV)
0.0	0.253	2.25	0.315
0.1	0.0381	2.50	0.231
0.2	0.0571	2.75	0.170
0.3	0.0838	3.00	0.132
0.4	0.124	3.25	0.104
0.5	0.177	3.50	0.0861
0.6	0.228	3.75	0.0777
0.7	0.282	4.00	0.0938
0.8	0.330	4.25	0.0682
0.9	0.363	4.50	0.0430
1.0	0.383	4.75	0.0232
1.25	0.427	5.00	0.0129
1.50	0.485	5.50	0.0030
1.75	0.424	6.00	0.0006
2.00	0.369	6.5	0.0

TABLE X
GAMMA-RAY PRODUCTION PROBABILITY FROM INELASTIC SCATTERING FROM ^{240}Pu
(Normalized to one photon per event)

E_γ (keV) \ E_0 (keV)	43.18	142.6	297.2	500.0	601.5	700.0	866.6	906.8	949.0	1090.0
43	1.000	1.000	0.5650	0.5507	0.5447	0.4117	0.3948	0.3878	0.3818	0.3740
99	-	0.0	0.4350	0.4482	0.4532	0.1438	0.0268	0.0228	0.0328	0.0436
154	-	-	0.0	0.0011	0.0022	0.0017	0.0018	0.0012	0.0006	0.0006
264	-	-	-	-	-	-	0.0	0.0108	0.0351	0.0732
304	-	-	-	-	-	-	-	0.0	0.0042	0.0110
556	-	-	-	-	0.0	0.2795	0.3626	0.3571	0.3133	0.2300
599	-	-	-	-	0.0	0.1633	0.2141	0.2113	0.1846	0.1347
761	-	-	-	-	-	-	-	0.0	0.0119	0.0250
820	-	-	-	-	-	-	0.0	0.0078	0.0203	0.0482
860	-	-	-	-	-	-	-	0.0	0.0119	0.0250
863	-	-	-	-	-	-	0.0	0.0012	0.0036	0.0064
902	-	-	-	-	-	-	-	-	0.0	0.0116
945	-	-	-	-	-	-	-	-	0.0	0.0168

TABLE XI
GAMMA-RAY MULTIPLICITIES FOR ^{240}Pu

$E_0 = 10^{-5}$ eV to 1.09 MeV

E_0 (keV)	Fission	Radiative Capture	Inelastic
Thermal	8.095	3.48	-
43.18	8.095	3.48	1.000
142.6	8.095	3.48	1.000
297.2	8.095	3.48	1.770
500.0	8.095	3.48	1.816
601.5	8.095	3.48	1.836
700.0	8.095	3.48	1.739
866.6	8.095	3.48	1.677
906.8	8.095	3.48	1.666
949.0	8.095	3.48	1.679
1090.0	8.095	3.48	1.722

TABLE XII
 GAMMA-RAY PRODUCTION CROSS SECTIONS FOR ^{240}Pu , IN BARNS/MeV

E_0 (MeV) \ E_γ (MeV)	1.09	2.1	3.0	4.0	5.0	6.0	7.5	14.8	20.0
0.0	8.79	9.94	8.23	12.35	11.87	11.80	12.50	9.69	8.09
0.1	13.48	11.31	10.12	15.20	13.73	13.96	15.11	12.74	11.52
0.2	15.88	12.85	12.26	17.39	16.11	16.32	18.14	15.51	14.18
0.3	16.08	14.04	14.73	20.14	18.79	18.49	22.20	18.46	16.53
0.4	15.29	15.23	16.30	21.18	21.45	20.39	24.28	20.50	18.60
0.5	14.39	15.14	16.54	21.38	21.95	20.94	25.02	21.24	19.36
0.6	12.91	14.50	15.97	19.28	20.26	19.96	23.97	20.31	19.33
0.7	10.94	12.95	13.33	15.20	15.81	16.41	19.80	18.64	18.22
0.8	8.84	11.22	10.86	11.68	12.36	12.10	13.86	15.23	16.45
0.9	7.17	9.39	9.04	9.40	9.39	9.14	10.74	12.28	13.91
1.0	5.79	7.93	7.66	7.46	7.41	7.28	8.75	10.15	11.63
1.25	3.79	5.01	5.18	4.56	4.64	4.89	5.62	6.66	7.39
1.50	2.68	3.19	3.70	3.21	3.31	3.74	4.07	4.67	5.21
1.75	1.90	2.11	2.90	2.48	2.49	3.18	2.99	3.28	3.59
2.00	1.50	1.50	2.24	2.02	2.11	2.60	2.23	2.40	2.60
2.25	1.17	1.14	1.69	1.70	1.71	2.08	1.72	1.76	1.84
2.50	0.902	0.884	1.21	1.34	1.33	1.61	1.31	1.29	1.32
2.75	0.708	0.696	0.873	1.02	0.989	1.27	1.01	0.955	0.950
3.00	0.551	0.557	0.568	0.712	0.702	0.982	0.792	0.711	0.689
3.25	0.430	0.439	0.388	0.497	0.548	0.751	0.618	0.551	0.519
3.50	0.340	0.349	0.305	0.361	0.434	0.581	0.480	0.425	0.401
3.75	0.269	0.277	0.239	0.285	0.344	0.435	0.373	0.330	0.311
4.00	0.215	0.220	0.190	0.226	0.274	0.339	0.287	0.259	0.248
4.25	0.169	0.175	0.152	0.180	0.217	0.254	0.227	0.204	0.196
4.50	0.131	0.138	0.121	0.142	0.172	0.199	0.173	0.161	0.159
4.75	0.105	0.111	0.096	0.113	0.137	0.155	0.136	0.127	0.126
5.0	0.082	0.088	0.075	0.089	0.109	0.124	0.103	0.099	0.102
5.5	0.052	0.054	0.047	0.056	0.069	0.079	0.064	0.064	0.064
6.0	0.033	0.035	0.030	0.036	0.043	0.050	0.038	0.040	0.041
6.5	0.020	0.022	0.019	0.022	0.028	0.031	0.024	0.025	0.026
7.0	0.012	0.014	0.012	0.015	0.018	0.019	0.016	0.015	0.017
8.0	0.0	0.0	0.0	0.0	0.0	0.0	0.0	0.0	0.0

TABLE XIII
 TOTAL GAMMA-RAY PRODUCTION
 CROSS SECTIONS FOR ^{240}Pu

E_0 (MeV)	$\int_0^{8 \text{ MeV}} \sigma(E_\gamma) dE_\gamma$ (barns)	$\int_0^{0.5 \text{ MeV}} \sigma(E_\gamma) dE_\gamma$ (barns)
1.09	16.68	7.22
2.1	17.80	6.60
3.0	18.66	6.58
4.0	21.80	9.07
5.0	21.86	8.69
6.0	22.52	8.55
7.5	25.08	9.85
14.8	23.76	8.25
20.0	23.63	7.44

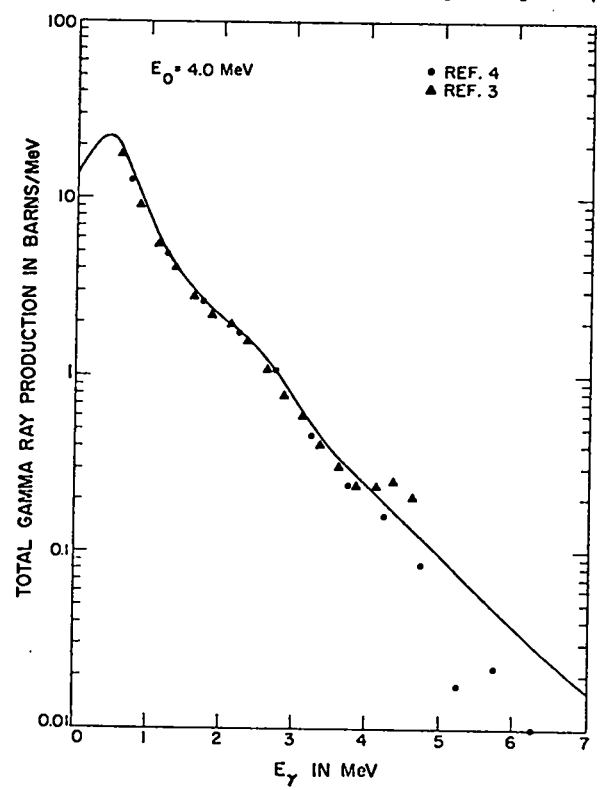
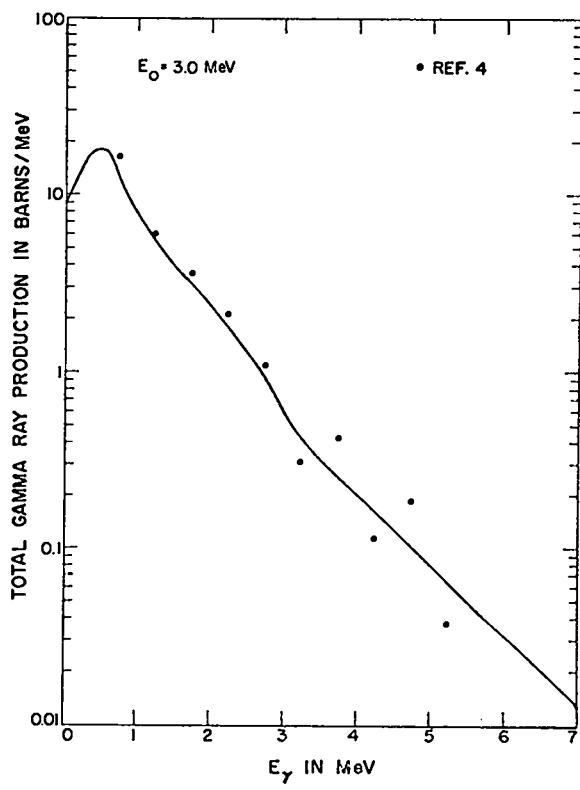
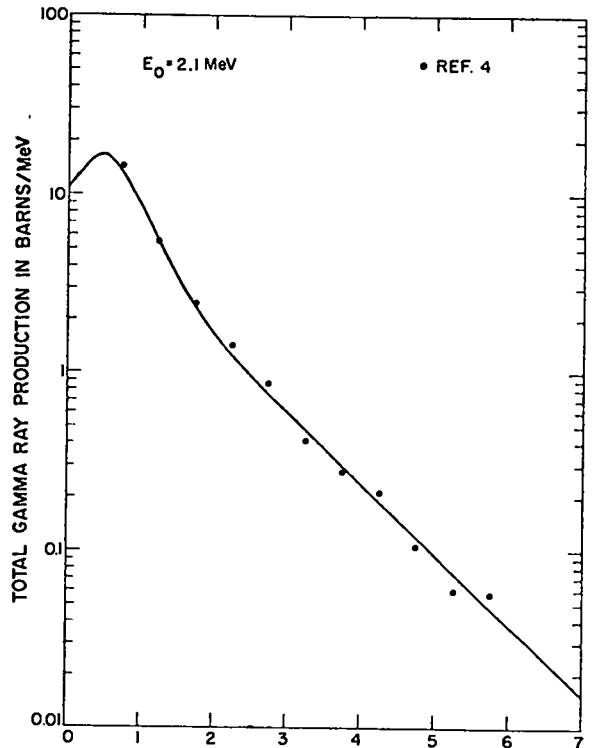
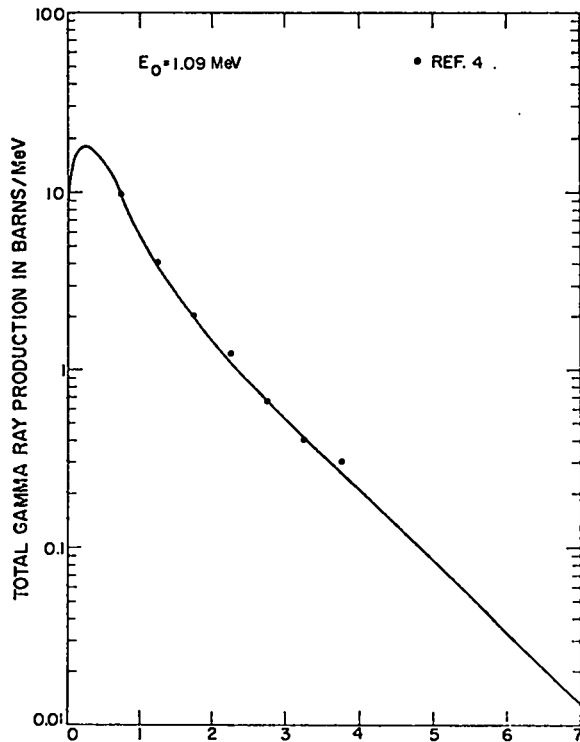


Fig. 4. Total gamma-ray production cross sections for ^{239}Pu in barns per MeV as a function of E_γ , for incident neutrons of 1.09, 2.1, 3.0, and 4.0 MeV.

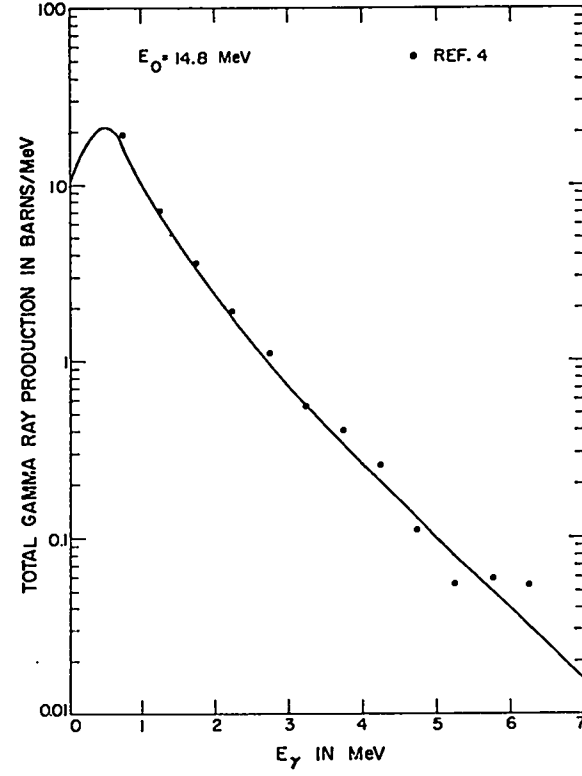
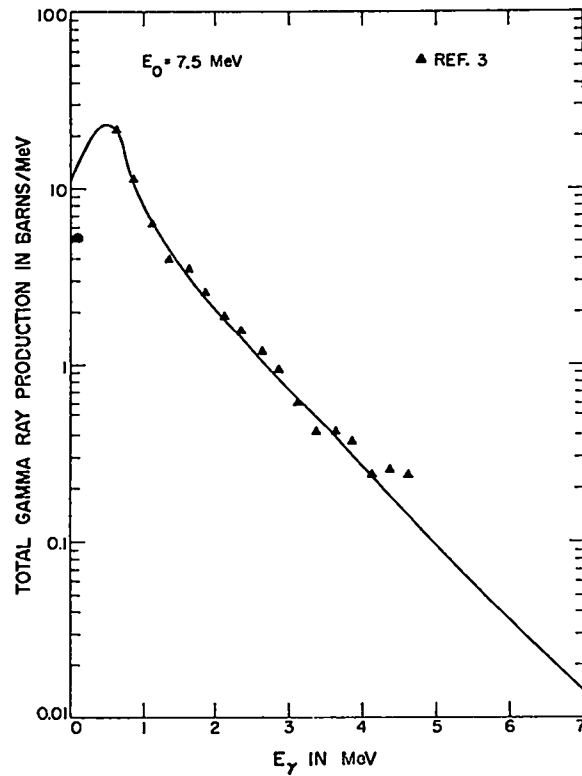
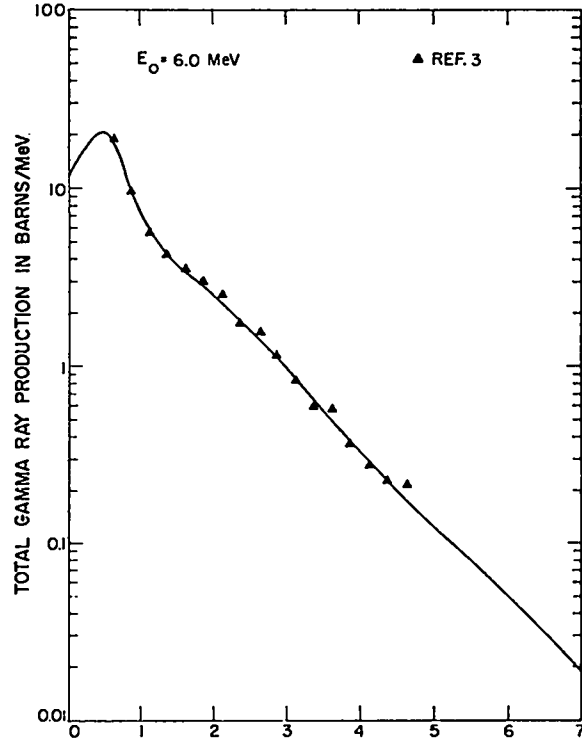
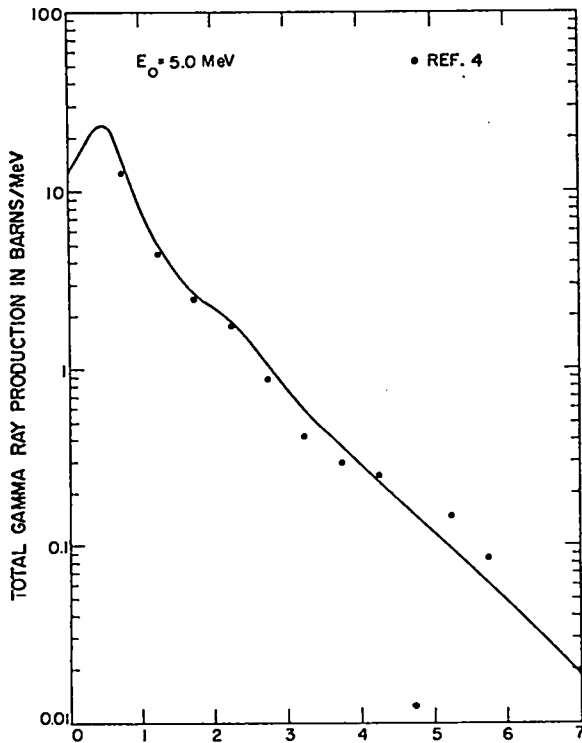


Fig. 5. Total gamma-ray production cross sections for ^{239}Pu in barns per MeV as a function of E_γ , for incident neutrons at 5.0, 6.0, 7.5, and 14.8 MeV.

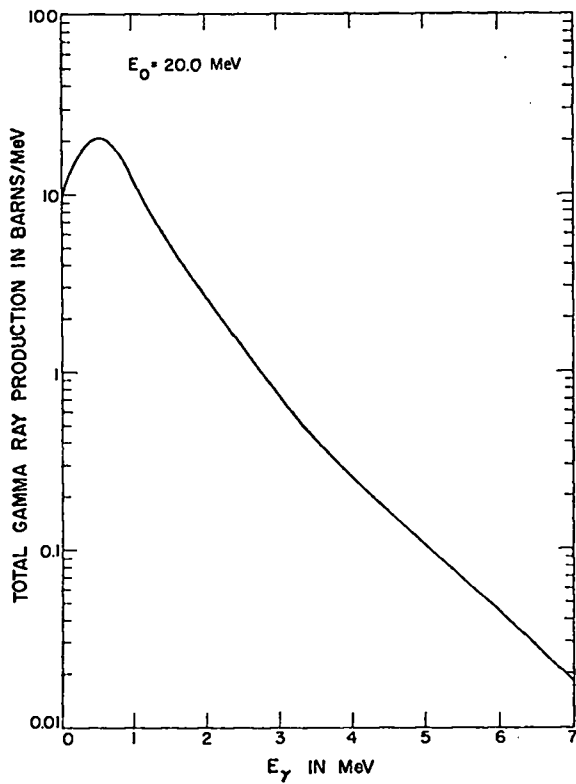


Fig. 6. Total gamma-ray production cross section for ^{239}Pu in barns per MeV as a function of E_γ , for incident neutrons of 20.0 MeV.

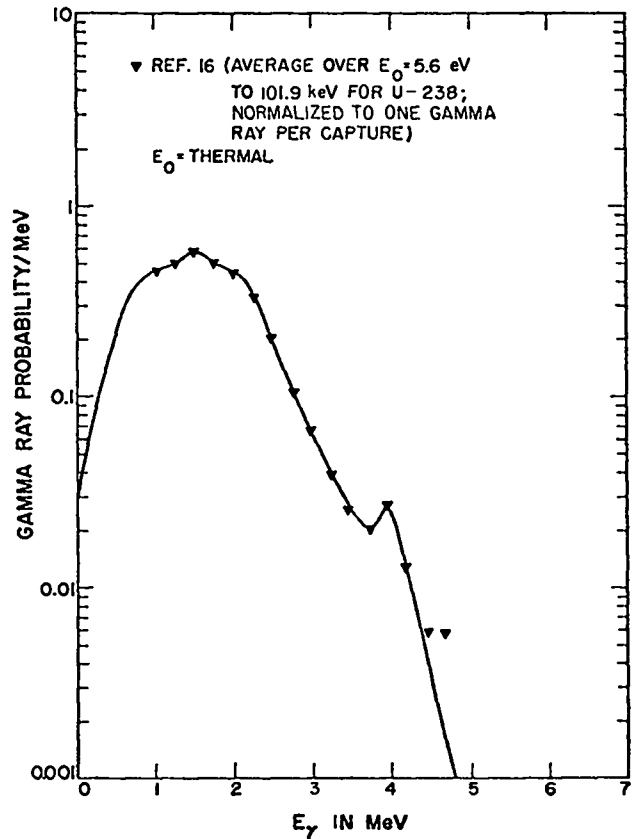


Fig. 7. Probability for production of photons as a function of E_γ due to capture by ^{240}Pu (normalized to 1 gamma ray per capture), for thermal neutrons. Values are from data¹⁶ on ^{238}U , averaged over incident neutron energies from 5.6 eV to 101.9 keV.

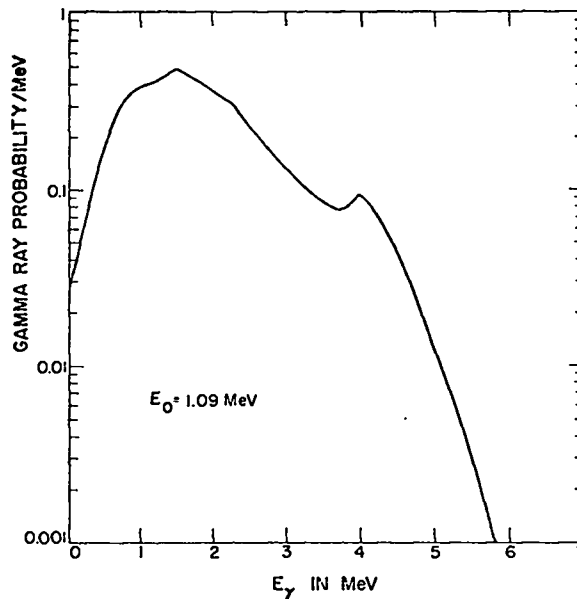


Fig. 8. Probability for production of photons as a function of E_γ due to capture by ^{240}Pu (normalized to 1 gamma ray per capture), for 1.09-MeV neutrons.

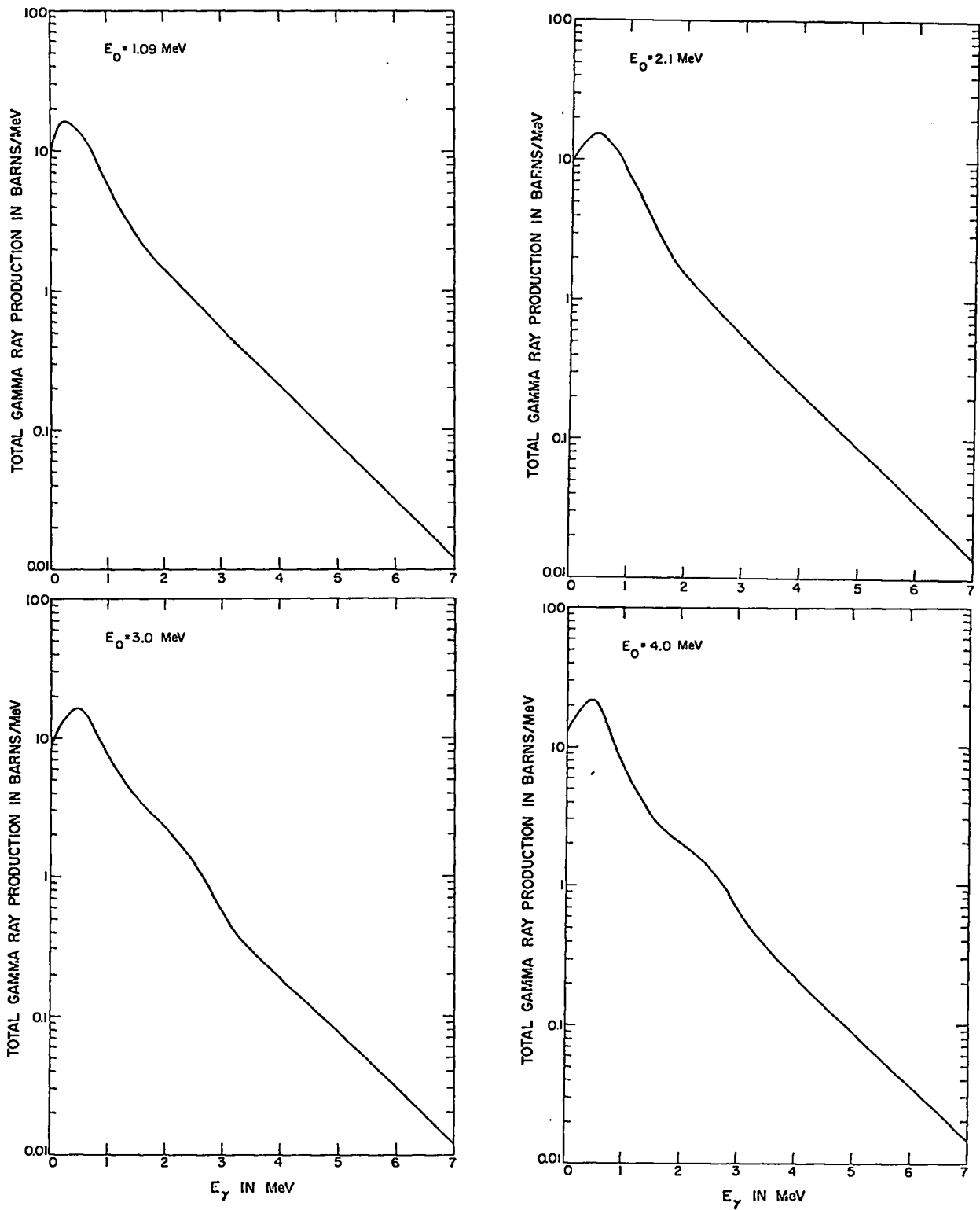


Fig. 9. Total gamma-ray production cross sections for ^{240}Pu in barns per MeV as a function of E_γ , for incident neutrons of 1.09, 2.1, 3.0, and 4.0 MeV.

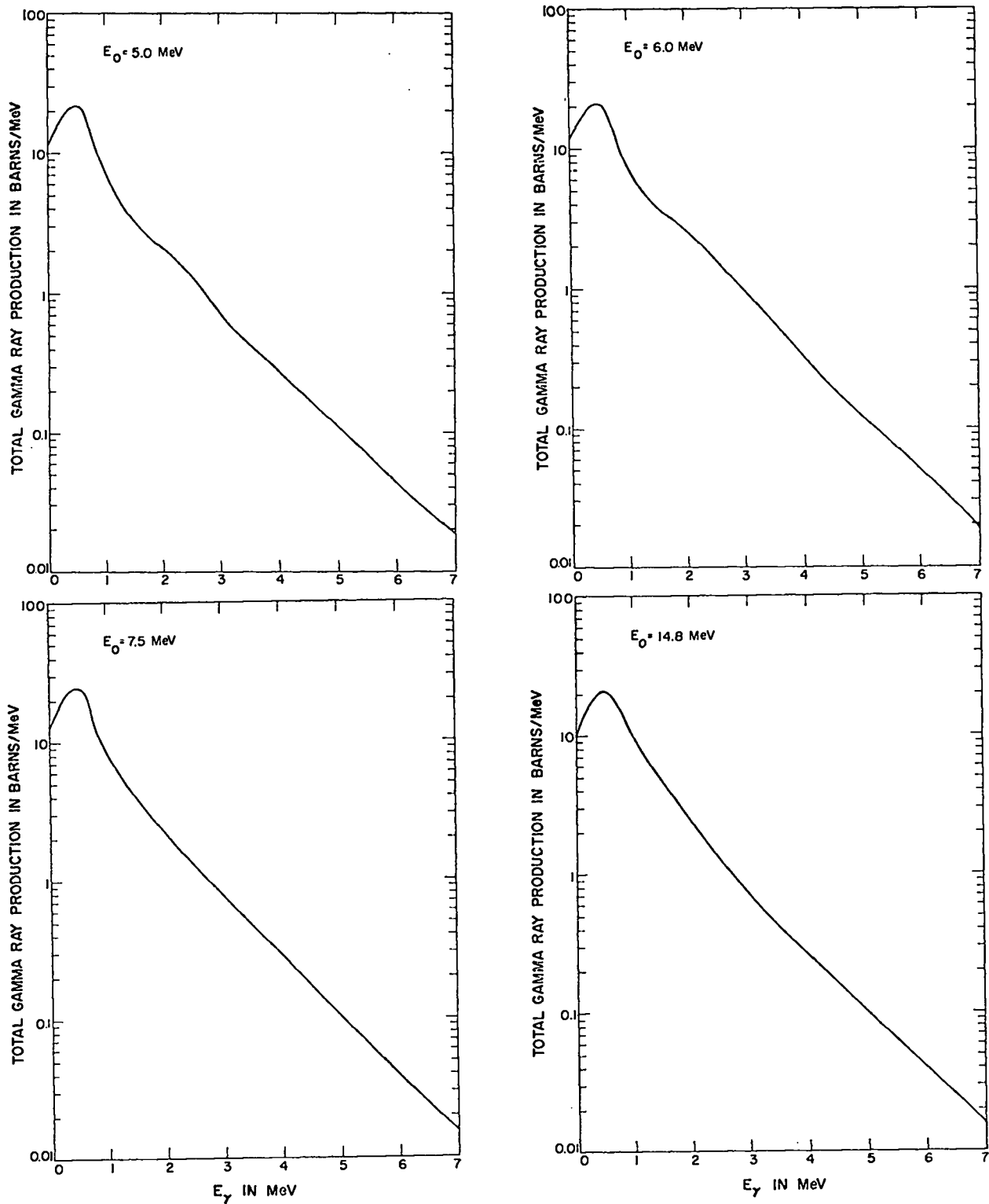


Fig. 10. Total gamma-ray production cross sections for ^{240}Pu in barns per MeV as a function of E_γ , for incident neutrons of 5.0, 6.0, 7.5, and 14.8 MeV.

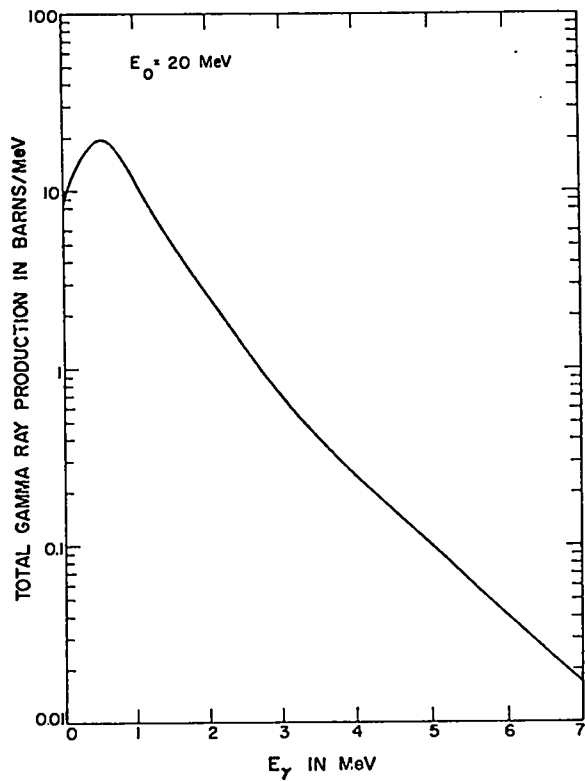


Fig. 11. Total gamma-ray production cross section for ^{240}Pu in barns per MeV as a function of E_γ , for incident neutrons of 20.0 MeV.

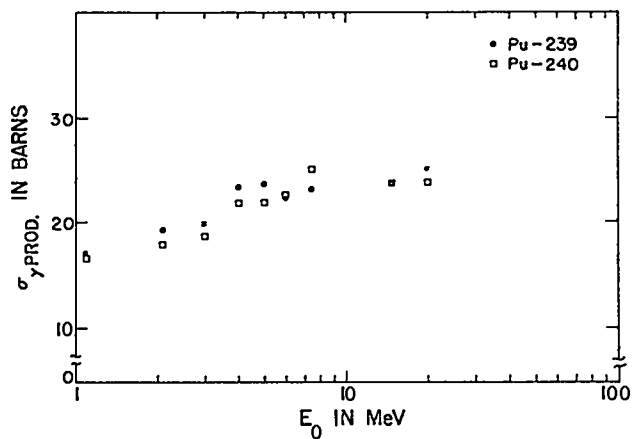


Fig. 12. Total gamma-ray production cross sections in barns for ^{239}Pu and ^{240}Pu as a function of incident neutron energy. All points shown are experimental except for the 20-MeV data on ^{239}Pu and all points on ^{240}Pu .